Conf-920672--3

A PERSPECTIVE ON TRANSITION TEMPERATURE AND K_{Jc} DATA CHARACTERIZATION*

D. E. McCabe, J. G. Merkle,† and R. K. Nanstad

Metals and Ceramics Division
OAK RIDGE NATIONAL LABORATORY
Oak Ridge, Tennessee 37831-6151

CONF-920672--3

DE93 003088

ABSTRACT

Proper identification of the transition temperature and the shape of the lower-bound (K_{Ic}) fracture toughness curve in the transition range has been a long-term objective of work at Oak Ridge National Laboratory. A past practice has been to test a large number of specimens of varying sizes, from 1/2T to 8T compacts, in expectation that size effects and statistical variability of K_{Jc} could be resolved empirically. Recently, statistical and constraint-based models have been developed that purport to explain much of what has been seen. Weakest-link theory has been successfully used to predict specimen size effects for the lower part of the transition curve. Constraint-based models of $\beta_c - \beta_{Ic}$ and J_{ssy} (small-scale yield) also can model size effects, but these tend to conflict among themselves with regard to the prediction of full constraint K_{Jc}. All lack potential for defining the absolute lower bound of fracture toughness. Statistically based models

*Research sponsored by the Office of Nuclear Regulatory Research, U.S. Nuclear Regulatory Commission, under Interagency Agreement DOE 1886-8011-9B with the U.S. Department of Energy under contract DE-AC05-84OR21400 with Martin Marietta Energy Systems, Inc.

†Engineering Technology Division.

DISCLAIMER

have the benefit of quantifying data scatter characteristics and provide a basis for making lower-bound toughness estimates with assigned error estimates. The appropriate characterization of transition temperature is of value in industrial problems and is of particular importance to the nuclear industry where safety issues are involved. Here the K_{Jc} data are obtained from small specimens, the size of which is dictated by volume limitations of surveillance capsule size. A basis has been explored for establishing a lower-envelope curve from such data.

INTRODUCTION

The procedures for measuring the plane strain fracture toughness, K_{Ic}, of metals were originally developed for relatively high yield strength materials, that generally are not strain rate sensitive. Values of fracture toughness measured with geometrically similar specimens were consistently observed to decrease with increasing specimen thickness, approaching an asymptotic minimum value. This behavior was attributed to the development of through-thickness tensile stresses, and the consequent elevation of the hydrostatic stress in the crack tip plastic zone, caused by the restraint against transverse contraction created by enforced compatibility with the surrounding elastic material. For fracture in the linear elastic range of the load-displacement curve, this behavior was controlled in order to obtain toughness values close to the lower asymptote by specifying specimen dimensions sufficiently large with respect to the plastic zone size at fracture. However, in the case of structural and pressure vessel steels, it is not always possible to test specimens large enough for fracture to occur under dominant linear-elastic conditions. Therefore, in these cases, the effects of large-scale yielding prior to fracture cannot be avoided, and since there presently is no analytical explanation, they are being treated empirically.

The empirical treatments of size effects on fracture toughness are of two types, statistical and phenomenological. The statistical treatments are based on the assumed existence of small-scale inhomogeneities that control the initiation of cleavage fracture. The resulting parameters are not entirely independent of temperature, and, for accuracy, the procedures may require more than the available number of specimens. Phenomenological approaches are based on the knowledge that yielding precedes the occurrence of cleavage microcracks and that the tensile ductility increases with decreasing hydrostatic stress. In addition, it is assumed that the hydrostatic stress decreases as the crack tip plastic zone size increases with respect to the distance to a free surface.

Early observations of size effects were made with center-cracked and edge-cracked plates, center-notched spin disks, notched beams, and circumferentially notched round bars. Using circumferentially notched round bar data to estimate K_{Ic}, Irwin [1] developed the following empirical equation based on the parameter β_{Ic} to estimate size effects in planar specimen data:

$$\beta_c = \beta_{Ic} + 1.4\,\beta_{Ic}^{\,3}\,, \tag{1}$$

where β = $(1/B)(K/\sigma_{ys})^2$.

B = specimen thickness, and

σ_{ys} = material 0.2% yield strength.

The notched round specimen was not adopted for general use because of problems concerning precracking, eccentricity, machine load capacity, and analysis. Instead, planar specimens loaded primarily in bending were found most practical, and size effects were avoided, at least for high yield strength low toughness materials, by applying conservative specimen size requirements.

The early approach taken in the testing of structural steels was to use only valid K_{Ic} values and to define the rising part of the transition curve so as to characterize the lower envelope of the fracture toughness data scatter. Specimen size requirements were difficult to satisfy, and data scatter among replicate tests was found to be about two to three times greater than that for ultrahigh strength materials. As a consequence, numerous tests were required, and, in the critical temperature range of rising toughness values where transition temperature is defined, prohibitively large specimens were required. Data scatter is also more accentuated. The ASME K_{Ic} design curve [2] shown in Fig. 1 serves as the primary example for such an approach. It can be noted that the critical rising toughness part of the transition range is defined with very few test results.

Most of the data shown are considerably above the lower-envelope K_{Ic} curve. Despite its tentative basis, the lower-bound curve shape, once hand-drawn and now mathematically approximated, is used in design and operation of nuclear reactors. In application, this curve is assumed to be of fixed shape for all pressure vessel steels and their weldments, and is translated up in temperature for irradiation damage effects using a reference temperature shift measurement, ΔRT_{NDT}, based on ASTM Standard Practice for Conducting Surveillance Tests for Light Water Cooled Nuclear Power Reactor Vessels (E 185-82).

A more recent approach to dealing with materials that display transition behavior is focused on the application of statistical modeling of data, such that specimen size effects and data scatter characteristics can be quantified. On the other hand, the practice of data censoring in the spirit of the valid K_{Ic} tradition is continuing, but K_{Ic} is being set aside in favor of more relaxed specimen size requirements. These new approaches are explored here.

CONSTRAINT ADJUSTMENTS

Constraint models suggest that the phenomenon of high data scatter and specimen size effects observed in the transition comes from an entirely different mechanism than the previously mentioned statistical models. The working hypothesis is that departure from the classical behavior of low data scatter and clear definition of lower-bound toughness observed with ultrahigh strength materials stems from loss of constraint. These models, therefore, collapse data scatter and predict a lowered toughness from large specimens.

Three closed-form equations have been proposed for adjusting small specimen fracture toughness data to estimate the lower values that would have been measured if the specimens had been under full constraint. Irwin's β_{Ic} adjustment [1],

$$K_c = K_{Ic}\sqrt{1 + 1.4\beta_{Ic}^2} \tag{2}$$

and a similar equation proposed by Hagiwara [3],

$$K_{Ic} = \frac{K_c}{\sqrt{1 + 2.3\sqrt{\beta_c}}} \tag{3}$$

are empirically based adjustments for thickness effects. Hagiwara's model was based on data from a structural steel, whereas Irwin's was based on data from ultrahigh strength materials. An equation for the toughness vs constraint relationship developed by Wallin [4], based on finite-element analyses of Anderson and Dodds [5] for a steel of Ramberg-Osgood work hardening exponent n = 10, is given as follows:

$$J/J_{ssy} = 1 + 176(J/B\sigma_{ys})^{1.37} . \tag{4}$$

Unlike the models of Eqs. (2) and (3), Eq. (4) is an elastic-plastic type of adjustment for loss of in-plane constraint, based on two-dimensional plane-strain finite-element calculations. Figure 2, adapted from a plot by Wallin [6], shows a comparison of the three-constraint adjustments mentioned above. The Dodds-Anderson-based curve of Eq. (4) was calculated for σ_{ys} = 517 MPa. A fourth curve is added by changing the coefficient in Eq. (2) from 1.4 to 0.224. This corresponds to changing the linear elastic fracture mechanics validity criterion from $\beta_{Ic} = 0.4$ to $\beta_{Ic} = 1.0$ [7]. For a range of β_c up to 64 [$K_J/(\sigma_{ys}\sqrt{B}) \leq 8$], the two original thickness-based adjustments of Irwin and Hagiwara reduce the toughness considerably more than the Dodds-Anderson in-plane adjustment. The modified Irwin adjustment curve lies close to the Dodds-Anderson curve until the latter curve passes through a maximum, with probably no physical significance, just beyond a recommended limit of $J/J_{ssy} = 4$. Figure 2 implies that as material toughness increases, constraint loss due to through-thickness contraction adds significantly to that due to in-plane effects. Figure 3 compares the predicted fracture toughness vs specimen size trend for the three models. All were applied to a baseline K_{Jc} toughness of 124.8 MPa√m in a 1/2T compact specimen. The lack of agreement is very evident.

TWO-DIMENSIONAL AND THREE-DIMENSIONAL ANALYSES

The development of practical procedures for quantifying constraint effects in the transition range is hampered by the lack of a proven general criterion for cleavage microcrack instability under multiaxial stress in the plastic zone just ahead of a crack tip. The problem is compounded by the difficulty of performing accurate three-dimensional elastic-plastic stress analyses near crack tips, especially considering the need to include finite strains and crack tip blunting in order to avoid calculating unrealistically high stresses. The mechanism by which constraint near a crack tip develops or relaxes has never been precisely described, but it is closely related to the fact that the sum of the principal plastic strains at a point must be zero and that not much plastic strain occurs in the direction of the intermediate principal stress unless it is equal to the minor principal stress. Near the surface of a through-cracked specimen the through-thickness stress is the minor principal stress and dimples in the surface within the plastic zone just ahead of the crack tip provide sure evidence of the negative plastic strains required to accommodate crack opening. However, in the mid-plane of the specimen, if the through-thickness stress is the intermediate principal stress, most of the negative plastic strain required to accommodate crack opening occurs in the forward direction, but this time accompanied by an elevation of the hydrostatic stress, especially if a neutral axis instead of a free surface is being approached. Eventually, as load increases, the through-thickness stress across the mid-plane becomes the minor principal stress, through-thickness contraction occurs more easily, and constraint is lost.

For conditions under which the through-thickness principal stress across the mid-plane near the crack tip is the intermediate principal stress, a two-dimensional elastic-plastic analysis may adequately describe the variation of constraint with load. On this basis, Anderson and Dodds [5] performed plane-strain finite-element analyses of notched beams with a/W ratios of 0.05, 0.15, and 0.50 and using a Ramberg-Osgood stress-strain relation. Small-scale yielding analyses of a circular domain containing an edge crack, loaded on its outer boundary by the displacements corresponding to linear elastic fracture mechanics mode I loading were also performed. In-plane relief of constraint in the beams was described by curves, for given values of a/W and n, relating J to J_{ssy}, where J is the value of the J-integral for the beam that produces the same area within a selected principal stress contour near the crack tip as does the smaller value of J_{ssy} in the small-scale yielding analysis. For $a\sigma_y/J > 200$, where σ_y is material flow stress, it was observed that J/J_{ssy} is close to unity, varying from about 1.05 for n = 5 to 1.25 for n = 50.

A three-dimensional analysis of a notched beam performed by Narasimhan and Rosakis [8] was used by Anderson and Dodds to confirm the recommendation of

$$B, b, a \geq 200(J_c/\sigma_y) \quad (5)$$

as a criterion for specimen dimensions sufficient to ensure relative size independence of cleavage fracture toughness.

The beam analyzed by Narasimhan and Rosakis had a thickness of 1 cm, a crack depth of 3 cm, a ligament length of 4.6 cm and a span of 30.5 cm. The material was a high-strength 4340 steel with a yield stress of 1030 MPa and a strain hardening exponent of 22. Because the ligament was thin relative to its length (B/b = 0.217), through-thickness constraint probably began to decrease at a relatively low fraction of the limit load. Nevertheless, Anderson and Dodds [5] made use of the calculated in-plane stress distributions on the assumption that deformation at the mid-plane remained in plane strain. Narasimhan and Rosakis calculated the three principal stresses vs position from the specimen mid-plane at distances from the crack tip ranging from 0.005 to 0.565 times the specimen thickness, for loads equal to 0.45, 0.7, and 1.0 times the calculated limit load. Anderson and Dodds selected one curve of opening mode stress vs lateral distance for each load, choosing distances of 1.56, 2.81, and 4.01 times the mid-plane crack tip opening displacement for the three loads, respectively, and normalizing the stresses by the mid-plane values. For each load, Anderson and Dodds calculated the parameter $B\sigma_y/J$, where σ_y is the flow stress, based on the Narasimhan and Rosakis plane-strain calculated values of $b\sigma_{ys}/J$, where b is ligament length and σ_{ys} is yield stress.

The successive values of $B\sigma_y/J$ were 235, 103, and 26.3. Because the normalized opening mode stress for the two lower loads were judged to be sufficiently fixed through at least 40% of the thickness of the specimen, the proposed size criterion of 200 J/σ_y was judged to be confirmed. Later, recalculation of the $B\sigma_y/J$ values based on the Narasimhan and Rosakis three-dimensional calculations of J produced lower values, with the highest being lower than 200, thus rendering the proposed criterion more conservative.

The assumption of plane strain at the mid-plane of the Narasimhan and Rosakis beams was apparently based on a close comparison between the angular variation of the near-tip in-plane stresses at all loads with that calculated from the plane-strain HRR solution, plus agreement between three-dimensional and plane-strain calculated values of opening mode stress at the mid-plane ahead of the crack tip. However, upon further examination of the Narasimhan and Rosakis analysis, it turns out that the through-thickness principal stress at the chosen reference distance is the intermediate principal stress at only the lowest of the three loads considered, and becomes the minor principal stress for the two higher loads. The through-thickness strains can also be estimated by using the equations of the deformation theory of plasticity. The plastic through-thickness strains are always negative, while the elastic strains start out positive. The former generally increase with load, but the latter decrease and eventually become negative as limit load is approached. Thus, the in-plane stresses at the mid-plane may be close to plane strain values, but the through-thickness stress and the hydrostatic stress are not necessarily so. Thus, if ductility and toughness are sensitive to hydrostatic stress, then constraint in small specimens loaded by necessity to fracture in the elastic-plastic range is likely to be significantly affected by three-dimensional effects.

The possibility that the through-thickness principal stress near the crack tip may change from being the intermediate to the minor principal stress as load increases is not completely proven by the above observations. This is because the reference distance chosen by Anderson and Dodds were increasing multiples of the crack tip opening displacement as load increased, and the analyses being examined were small strain analyses. At fixed distances from the crack tip, the order of the principal stresses did not change. The through-thickness stress, σ_{zz}, is always σ_2 at r/B = 0.005 and is always σ_3 at r/B = 0.125. Thus, the through-thickness principal stress is the intermediate principal stress only close to the crack tip, and how the order of the principal stresses changes with load in this region needs to be more completely examined with incremental large strain calculations.

STATISTICAL METHODS

In the early 1970s, Landes and Shaffer [9] introduced a statistically based discipline for the evaluation of transition range J_c data that utilizes all the test information and is not limited by having to satisfy validity requirements for pure plane-strain constraint. Instead, J-integral at the onset of cleavage crack instability, J_c, is determined and used to define statistical distributions for replicated data sets of fracture toughness. The Weibull cumulative frequency distribution function is used to fit these J_c distributions. In addition, the experimentally observed tendency for large specimens to have lower mean toughness than smaller ones was noted and a weak-link statistical theory was incorporated to explain the trend. Initially, a two-parameter Weibull function of the following form was used:

$$P_f = 1 - \exp - (J/\theta)^b \,, \tag{6}$$

where P_f = probability that a sample specimen selected from a population will have J_c toughness less than or equal to J,

b = Weibull slope, and

θ = toughness scale factor (J at $P_f = 0.632$).

The weak-link size effect was incorporated in the form of the operator on the scale factor, θ, as follows:

$$J_\theta = \theta/(B_x/B_o)^b \,, \tag{7}$$

where J_θ replaces θ in Eq. (6),

B_x = thickness of J_c prediction, and

B_o = thickness of test specimens used to determine the Weibull constants.

It was later recognized that the two-parameter Weibull model had no lower bound for toughness prediction as thickness B_x approached infinity. In a follow-up paper by Landes and McCabe [10], three-parameter Weibull was introduced. Here, the value of J in Eq. (6) is replaced with $(J - J_{min})$, and θ with $(\theta - J_{min})$, so that J_θ is redefined as:

$$J_\theta = (\theta - J_{min})/(B_x/B_o)^b \ . \tag{8}$$

In this case, J will approach J_{min} as P_f approaches zero. All three parameters can be established from experimental data by ranking data according to increased values of toughness and then assigning probability values derived from statistical ranking formulae (see the following section). These values are then converted into Weibull variables via the following transformations:

$$Y = \ln[-\ln(1 - P)] \ . \tag{9a}$$

$$X = \ln(J_c - J_{min}) \ . \tag{9b}$$

The best linear fit to these data is made through the use of J_{min} as an independent variable. Example cases were worked [10] with partial success. However, these example determinations usually had only a few replicate test data and the sensitivity needed to develop accurate results was not available at that time.

Followup work by Wallin [11,12] incorporated many more data sets and far more data replications. Because of this, the author was able to identify some interesting properties of such data populations. The toughness parameter of choice was K_{Jc}, which, for elastic-plastic conditions, is a stress intensity factor derived from J_c via $\sqrt{J_c E}$. In Eqs. (6) through (8) above, K replaces J and the Weibull constants differ accordingly. It appeared that the Weibull slope tended to be a constant value near 4, and an apparently constant K_{min} value of near 20 MPa$\sqrt{m}$ was obtained through a sensitivity study. These constants were found to work suitably over a range of specimen sizes and test temperatures.

There are two major advantages to having two predetermined constant Weibull parameters. One is that the scale factor is the only unknown to be determined from test data, and in this case, relatively few specimens are required to make an accurate determination. The second advantage is that single toughness determinations can be transposed from one specimen size to another because weakest-link theory reduces to the following simple relationship:

$$K_{Jcx} = 20 + (K_{Jco} - 20)\,(B_x/B_o)^{1/4}\,, \qquad (10)$$

where K_{Jcx} = predicted K_{Jc} for specimen of thickness, B_x, and

K_{Jco} = toughness of specimen of thickness, B_o.

PROBABILITY FUNCTIONS

In order to graphically or numerically make a direct estimate of the parameter, P_f, for a chosen cumulative probability function that best describes the variability of a given set of data, it is first necessary to assign an estimated cumulative probability to each data value. In principle, this step could be avoided by using nonlinear curve-fitting procedures to fit a probability density function to the histogram of data. However, it is usually much more convenient to graphically or analytically linearize the relationship between cumulative probability and the variable, in which case estimated cumulative probabilities are required. There are two mathematical bases for estimating cumulative probability for ordered data. The first is an approach based on expected values [13], which leads to the formula:

$$P_f = i/(N + 1)\,, \qquad (11)$$

where N is the number of values in the data set and i is the order number counting from the smallest to the largest. The second approach is based on the recognition that any one sample of N numbers is only one of an infinite number of such samples [14]. In order to have equal probabilities of over- or underestimating cumulative probabilities, an equation for determining median probabilities has been derived [14,15]. The equation is somewhat complicated, but can be closely approximated by the following formula [15,16]:

$$P_f = (i - 0.3)/(N + 0.4) \ . \qquad (12)$$

Other approximate formulae of the same form exist [17]. Equation (12) has been selected for use in a draft transition range standard submitted to ASTM Task Group E24.08.08.

WEIBULL MODEL FITTING

The ideal example of fitting data with the two fixed parameters of slope = 4 and K_{min} = 20 MPa$\sqrt{m}$ is shown in Fig. 4 for 2T compact specimens of A 533 grade B steel tested in the mid-transition and on the lower shelf. Another example that covers specimen size effects is shown in Fig. 5. These examples essentially confirm Wallin's observation that fracture toughness data distributions are of fixed shape (i.e., fixed Weibull slope). It should be understood, however, that occasionally some data sets may not show the best fit using these two constants, but such departures seldom develop in a pattern or have consistency of occurrence such that an alternate or more suitable model can be suggested.

Recently, experiments with large numbers of replicate tests have been run in order to verify the results of earlier sensitivity studies. Previously, Monte Carlo techniques had been used to artificially generate the data needed to establish the two fixed Weibull parameters. Instead of obtaining clear experimental confirmation, a puzzling pattern was observed. Data at the low toughness end of a distribution tended to drop down from the fixed slope of 4 as illustrated in Fig. 6. These data came from a Materials Properties Council round-robin activity [18] involving 13 laboratories that tested 1T compact specimens of an A 508 steel at three temperatures (–100, –75, and –50°C). Seven laboratories, each of which tested five replicates, contributed to Fig. 6. The dropoff was observed at all three test temperatures to varying degrees. To prove that the pattern was not due to bias from a single laboratory, the one participant that produced the lowest ranked toughness K_{Jc} value was singled out and evaluated alone (see Fig. 7). The dropoff was not evident in this data set. The median K_{Jc} for this laboratory's data was 157.7 MPa√m and the grand median over all laboratories was 159.7 MPa√m. The next evaluation tried was to view original data as a histogram. Data at –50°C were selected to compare with the density function curve from the Weibull fit (see Fig. 8). The histogram suggests that the data tend to cluster somewhat in the low-toughness region, displaying less of a "tail" than in the high-toughness region. The conclusion drawn from this was that there is an influence of real material lower-bound toughness that appears only in large data sets. Current evidence suggests that the physical lower bound is greater than the mathematical constant K_{min} of 20 MPa√m that works well in Weibull fitting. Therefore, it appears that the three-parameter Weibull distribution function can be fitted to the dominant portion of K_{Jc} data, but the clustering observed in the lower tail of a statistically well-defined data distribution cannot be characterized mathematically.

CRACK GROWTH CORRECTION

Slow-stable crack growth prior to the onset of cleavage cracking is, for various hypothetical reasons, reputed to cause a disruption of the local crack tip stress field. Ostensibly, the propensity for onset of cleavage fracture is changed from that of a specimen with a nongrowing crack. One argument has an empirical basis, suggesting that the propensity for cleavage cracking is reduced by loss of crack tip constraint due to cross slip deformation. The result is a sharp drop in Weibull slope as seen in Fig. 9.

Statistical models, on the other hand, consider the extra volume of material that is introduced to cleavage activation level stresses by the advancing crack tip. Weakest-link theory suggests that the key elements are crack advancement distance and the size of the zone of high stress that is a linear function of plastic zone development. The first model, developed by Bruckner and Munz [19], incorporated R-curve effects with some complexity. Wallin [20] has produced a simplified correction factor defined as follows:

$$\text{Corr.} = [1 + (2\Delta a\sigma_y^2)/(\gamma K_{Jc}^2)]^{1/4} . \qquad (13)$$

Parameter γ is a normalized length factor that is related to the distance from the crack tip to the point of maximum stress ahead of the tip. The correction factor is applied as a multiplying factor to Eq. (10) in an identical manner as the weakest-link theory for specimen thickness.

$$K_{Jcx} = 20 + [K_{Jco} - 20]\,(B_x/B_o)^{1/4}\,[1 + (2\Delta a\sigma_y^2)/(\gamma K_{Jc}^2)]^{1/4}. \tag{14}$$

DATA ADJUSTMENT PRACTICE

Physical evidence had been presented in Fig. 9 that crack growth has altered the cleavage fracture behavior of A 36 steel bend bars. Several data sets of other materials that suffered intermediate onset of stable ductile crack growth have been similarly evaluated, but these did not show a change of Weibull slope. This apparent contradiction can be explained by combining the two known K_{Jc} data correction computations (see also ref. 4). Each datum can be adjusted by applying Eq. (4) for in-plane constraint loss and Eq. (14) for weakest link effect. To illustrate, data were taken from the Heavy-Section Steel Irradiation (HSSI) Program Fifth Irradiation Series [21], which were ideal for this evaluation because there were both variable specimen sizes (1T, 2T, 4T, 6T, and 8T) and test temperatures (–75, –50, –30, –15, –5, 0, and 5°C). The tests made above –15°C gave data points for an R-curve based on K_{Jc} data and slow stable growth to instability (see Table 1 and Fig. 10). Adjustments for constraint and for crack growth were applied to each datum according to the above-stated order with the results being as shown in

Fig. 11. The net result in this case is that the competing mechanisms of in-plane constraint loss and increased sampling volume tend to analytically cancel each other out. Therefore, if both adjustment models are accurate, it would seem that data with crack growth can be accepted as sufficiently accurate without adjustment, for many cases. On the other hand, there can be circumstances where one of the two competing mechanisms is absent. For example, the constraint adjustment can be applied below the J_{Ic} toughness level and there will be no cancellation due to crack growth. However, as illustrated in Fig. 11, when the constraint adjustment is applied in the absence of stable crack growth, the Weibull slope is increased to an artificially high level. Such a slope change is almost never seen experimentally in tests with large specimens. Alternatively, very large specimens can be tested at high temperatures, where there will be crack growth under essentially small-scale deformation, in which case the crack growth adjustment is applied in the absence of counteracting constraint loss. Hence, the value of adjustment practices in their current state of development is not currently known.

LOWER-BOUND TOUGHNESS BY STATISTICAL METHODS

The ASME lower-envelope K_{Ic} curve in Fig. 1 has been in use for many years in setting safe operating limits for reactor vessels and for safety assessments in hypothetical accident scenarios. This curve has been widely accepted, despite the fact that no precise statistical significance has been established for the location of the lower bound. A set of data similar to that of Fig. 1 has been developed under well-controlled conditions in the HSSI Fifth Irradiation Series, such that a good illustrative demonstration of statistical methods could be made. Specimens of A 533 grade B weld metal covering a wide range of compact specimen sizes and a consistent pattern of test temperatures were used. These data had been shown [21] to be either on or above the ASME lower-envelope curve. Nevertheless, it was of interest to use the data again to see what the currently available statistically based working theories indicate. The following theories will be employed:

1. Data obtained from various specimen sizes can be transposed to a 1T compact specimen size equivalence, using Eq. (10).

2. The three-parameter Weibull distribution function with fixed slope of 4 and fixed K_{min} of 20 MPa√m is used to fit data populations for each test temperature.

3. A master curve developed by Wallin [22] will be used to model the trend of median K_{Jc} values over all test temperatures. The master curve is defined by the following equation:

$$K_{med} = 30 + 70 \exp[0.019(T - T_o)] \, , \tag{15}$$

where T_o is the characteristic temperature defined at $K_{Jc(med)}$ = 100 MPa√m.

The above positioning of the K_{Jc} median transition curve based on T_o is much the same as the positioning of the lower-bound K_{Ic} curve based on the RT_{NDT} temperature.

4. The standard deviation of a data population is known to be a function of the Weibull slope and the median toughness K_{Jc}. When the Weibull slope is 4, the standard deviation is

$$\overline{\sigma} = 0.28\ K_{Jc(median)}\ [1 - 20/K_{Jc(median)}]\ . \qquad (16)$$

The standard normal deviation for one tail of a distribution at 95% confidence is 1.64.

The forgoing four relationships, applied to the HSSI Fifth Irradiation Series data, produce the result shown in Fig. 12. The particular lower-bound curve shown in Fig. 12 seems to have the correct position and curve shape for a 95% confidence fit. Wallin [22] and Stienstra [16] have shown equally good results with other data available in the literature. The ASME lower-bound curve, shown for comparison, tends to be the same up to the mid-transition, but tends to be less conservative as the upper shelf is approached.

CONCLUSIONS

The purpose of this paper was to provide a perspective on the transition range fracture toughness data evaluation concepts that have been developed in recent years.

Data evaluation for lower-bound toughness determination is no longer restricted by having to meet K_{Ic} validity requirements. New elastic-plastic analysis tools are under development, and statistical methods have been developed that will allow more productive use of test data.

Constraint models postulate that K_{Jc} data taken from relatively small test specimens lack the constraint control of large specimens. All project a trend of toughness vs size mathematically so that size effects can be eliminated through data adjustment. Three basic constraint-based models were examined and two observations were made: (1) the available models for predicting full constraint toughness do not agree with each other, and (2) it is uncertain that the low envelope type of toughness representation can ever be defined by using deterministic-type methods on data of high intrinsic variability.

Dodds and Anderson have used two-dimensional finite-element analyses and the assumption of plane-strain constraint to set specimen dimension requirements so as to achieve size independence of cleavage fracture. It was concluded that these analyses, although good on a qualitative basis, lacked critical refinement of crack tip stress analysis to understand fully all of the constraint implications. Three-dimensional large-strain analysis is needed to support the claim of small-scale yielding, under dominant plane strain for $B \geq 200\ J/\sigma_y$.

A three-parameter Weibull model with a fixed slope of 4 and K_{min} = 20 MPa√m seems to fit most K_{Jc} data distributions. However, data sets with extensive replications tend to cluster at the low toughness end of the distribution. This phenomenon is associated with the presence of a material minimum toughness or a true lower bound. These minimums are almost always greater than the 20 MPa√m used in three-parameter Weibull fitting. Currently, there is no modification to a Weibull distribution that will satisfactorily model clustered data. Until one is developed that does not require an unreasonably large number of specimens for data fitting, there will not be a practical way to include this aspect of transition range fracture toughness behavior in standard procedures.

The adjustment of K_{Jc} data that involve slow-stable crack growth involves both a correction for constraint loss and a modified weakest-link model to account for the extra volume of material exposed to cleavage level stresses. These are opposing effects that tend to cancel each other. The net result is that the Weibull slope should not change in most cases for toughness values above the value of K corresponding to J_{Ic}.

Data from the HSSI Fifth Irradiation Series were used to demonstrate how statistical methods can be used for the determination of lower-bound toughness. At high toughness, the ASME lower-bound K_{Ic} curve tends to be less conservative than a statistically based curve. Considerable progress has been made in recent years toward the understanding of transition range fracture toughness data, and more is expected to be made in the near future.

ACKNOWLEDGMENTS

This work has been supported by the U.S. Nuclear Regulatory Commission through the Heavy-Section Steel Technology Program. Their continued support for the development of this technology is greatly appreciated. The manuscript was prepared by J. L. Bishop and her contribution is appreciated.

REFERENCES

[1] Irwin, G. R., "Fracture Mode Transition for a Crack Traversing a Plate," *Journal of Basic Engineering*, Vol. 82, No. 2, June 1960, pp. 417-425.

[2] "PVRC Recommendations on Toughness Requirements for Ferritic Materials," *WRC Bulletin 175*, Welding Research Council, August 1972.

[3] Hagiwara, G., "Evaluation of Thickness Effect on Fracture Toughness in Heavy Section Steels," Second Japanese-German Joint Seminar on Nondestructive Evaluation and Structural Strength on Nuclear Power Plants, Tokyo, Japan, February 1983.

[4] Wallin, K., "Statistical Aspects of Constraint with Emphasis to Testing and Analysis of Laboratory Specimens in the Transition Region," ASTM Symposium on Constraint Effects in Fracture, Indianapolis, Ind., May 8-9, 1991 (to be published).

[5] Anderson, T. L., and Dodds, Jr., R. H., "Specimen Size Requirements for Fracture Toughness Testing in the Transition Region," *Journal of Testing and Evaluation*, Vol. 19, No. 2, March 1991, pp. 123-134.

[6] Wallin, K., "The Size Effect on K_{Ic} Results," *Engineering Fracture Mechanics*, Vol. 22, No. 1, 1985, pp. 149-163.

[7] Merkle, J. G., *An Examination of the Size Effects and Data Scatter Observed in Small-Specimen Cleavage Fracture Toughness Testing*, NUREG/CR-3672 (ORNL/TM-9088), U.S. Nuclear Regulatory Commission, April 1984.

[8] Narasimhan, R., and Rosakis, A. J., *Three-Dimensional Effects Near a Crack Tip in a Ductile Three Point Bend Specimen - Part I: A Numerical Investigation*, SM 88-6, Division of Engineering and Applied Science, California Institute of Technology, Pasadena, Calif., January 1988.

[9] Landes, J. D., and Shaffer, D. H., "Statistical Characterization of Fracture in the Transition Region," *Fracture Mechanics: Proceedings of the Twelfth National Symposium on Fracture Mechanics, ASTM STP 700*, American Society for Testing and Materials, Philadelphia, 1980, pp. 368-382.

[10] Landes, J. D., and McCabe, D. E., "Effect of Section Size on Transition Temperature Behavior of Structural Steels," *Fracture Mechanics: Fifteenth Symposium, ASTM STP 833*, American Society for Testing and Materials, Philadelphia, 1984, pp. 378-392.

[11] Wallin, K., "The Scatter in K_{Ic} Results," *Engineering Fracture Mechanics*, Vol. 19, No. 6, 1984, pp. 1085-1093.

[12] Wallin, K., "Statistical Modelling of Fracture in the Ductile to Brittle Transition Region," *Defect Assessment in Components - Fundamentals and Applications*, ESIS/EGF9, Mechanical Engineering Publications, London, 1991.

[13] Mood, A. M., *Introduction to the Theory of Statistics*, McGraw-Hill, New York, 1950.

[14] Johnson, L. G., "The Median Ranks of Sample Values in their Population with an Application to Certain Fatigue Studies," *Industrial Mathematics*, Vol. 2, 1951, pp. 1-9.

[15] Johnson, L. G., *The Statistical Treatment of Fatigue Experiments*, Elsevier, New York, 1964.

[16] Stienstra, D. I. A., *Stochastic Micromechanical Modeling of Cleavage Fracture in the Ductile-Brittle Transition Region*, Ph.D. Thesis, Texas A & M University, College Station, Texas, August 1990.

[17] Neville, D. J., and Knott, J. F., "Statistical Distributions of Toughness and Fracture Stress for Homogeneous and Inhomogeneous Materials," *Journal of the Mechanics and Physics of Solids*, Vol. 34, No. 3, 1986, pp. 243-291.

[18] Van der Sluys, W. A., and Miglin, M. T., "Results of the MPC/JSPS Testing Program in the Brittle-to-Ductile Transition Region," 24th National Symposium on Fracture Mechanics, Gatlinburg, Tenn., June 30-July 2, 1992 (to be published).

[19] Ehl, W., Munz, D., and Bruckner, A., "Crack Extension in the Ductile-Brittle Transition Region," *Seminaire International sur L'Approche Local de la Rupture, Moret-sur-Loing*, June 1986, pp. 233-242.

[20] Wallin, K., "The Effect of Ductile Tearing on Cleavage Fracture Probability in Fracture Toughness Testing," *Engineering Fracture Mechanics*, Vol. 32, No. 4, 1989, pp. 523-531.

[21] Nanstad, R. K., McCabe, D. E., Menke, B. H., Iskander, S. K., and Haggag, F. M., "Effects of Radiation on K_{Ic} Curves for High-Copper Welds," *Effects of Radiation on Materials: Fourteenth International Symposium (Volume II), ASTM STP 1046*, American Society for Testing and Materials, Philadelphia, 1990, pp. 214-233.

[22] Wallin, K., "A Simple Theoretical Charpy V-K_{Ic} Correlation for Irradiation Embrittlement," *Innovative Approaches to Irradiation Damage and Fracture Analysis*, Vol. 170, proceedings of ASME Pressure Vessels and Piping Conference, held at Honolulu, Hawaii, July 23-27, 1989, American Society of Mechanical Engineers, New York, 1989.

Table 1. Example calculations of combined constraint and crack growth corrections applied to K_{Jc} data for unirradiated A 533 grade B weld metal

Compact specimen size	K_{Jc} (MPa√m)								
	−30°C			−15°C			−5°C		
	Before correction	Δa (mm)	After correction	Before correction	Δa (mm)	After correction	Before correction	Δa (mm)	After correction
1T	128.3	0.09	129.4	153.3	0.10	148.1			
	173.8	0.17	166.0	246.1	0.55	216.3			
2T	118.8	0.08	126.4	143.6	0.15	154.3	147.1	0	140.8
	127.4	0	123.6	165.9	0.19	174.7	214.8	0.33	217.2
4T	113.1	0	112.1	105.8	0	105.1	174.9	0.15	184.2
	176.6	0.18	187.3	156.6	0.14	167.8	221.4	0.45	241.6

LIST OF FIGURES

Fig. 8. Weibull probability density function compared to histogram of K_{Jc} data for MPC round robin data taken at −50°C.

Fig. 9. Weibull plot of K_{Jc} data for A 36 steel tested at −43°C. Open data points have slow-stable crack growth prior to instability.

Fig. 10. Resistance curve developed from K_{Jc} data over several specimen sizes for HSSI Fifth Irradiation Series. Unirradiated weld metal 73W at several different temperatures.

Fig. 11. Weibull plots for HSSI Fifth Irradiation Series unirradiated weld metal 73W, with no corrections, a correction for constraint only, and corrections for both constraint and stable crack growth.

Fig. 12. Data from HSSI Fifth Irradiation Series normalized to 1TC(T) equivalent data. Median curve fit, 95% lower-bound curve, and ASME lower-bound curve for RT_{NDT} = −34°C.

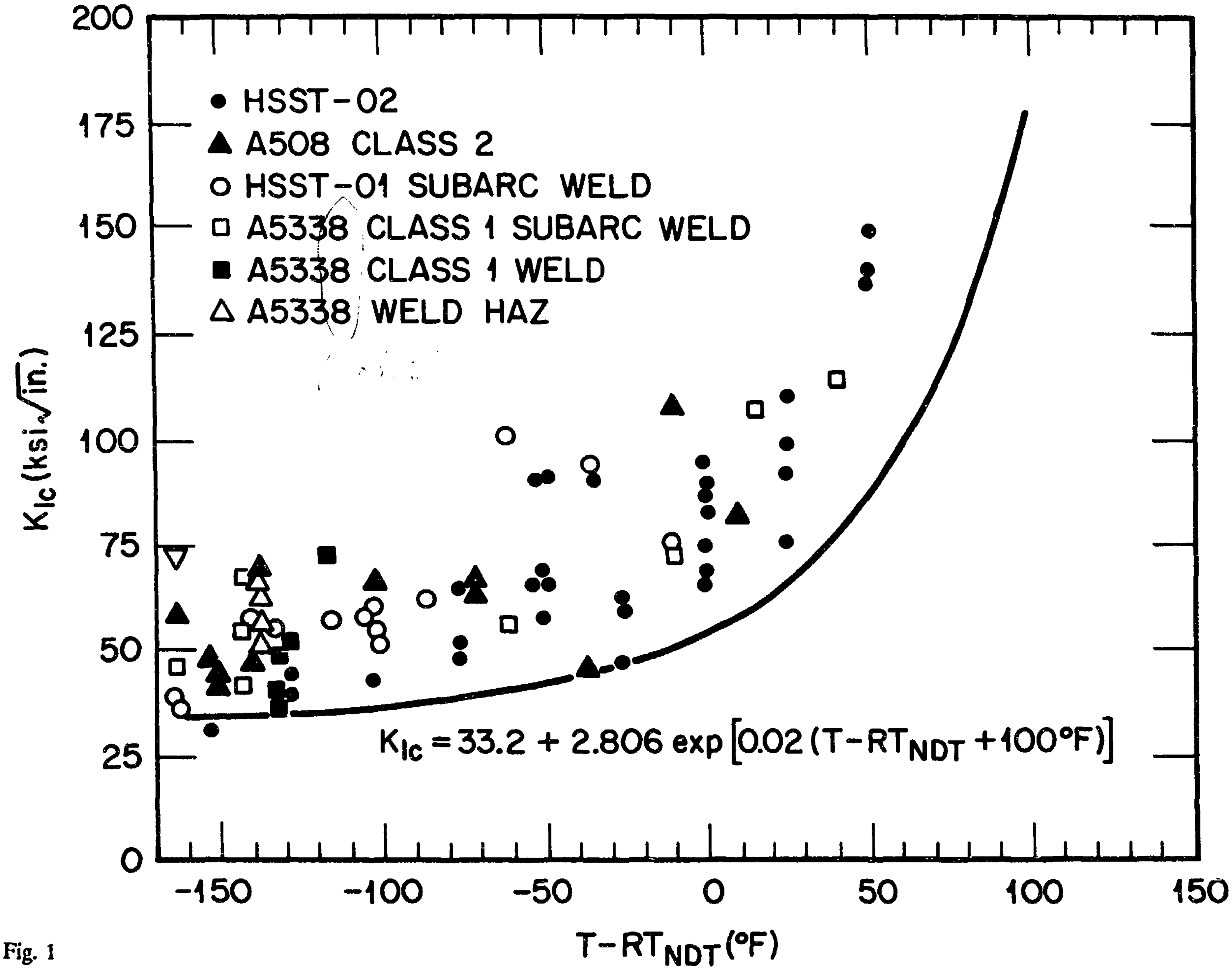

200
175
150
125
100
75
50
25
0
● HSST-02
▲ A508 CLASS 2
○ HSST-01 SUBARC WELD
□ A5338 CLASS 1 SUBARC WELD
■ A5338 CLASS 1 WELD
△ A5338 WELD HAZ
K_{Ic} (ksi $\sqrt{in.}$)
$K_{Ic} = 33.2 + 2.806 \exp[0.02(T-RT_{NDT}+100°F)]$
-150
-100
-50
0
50
100
150
$T-RT_{NDT}$ (°F)

Fig. 1

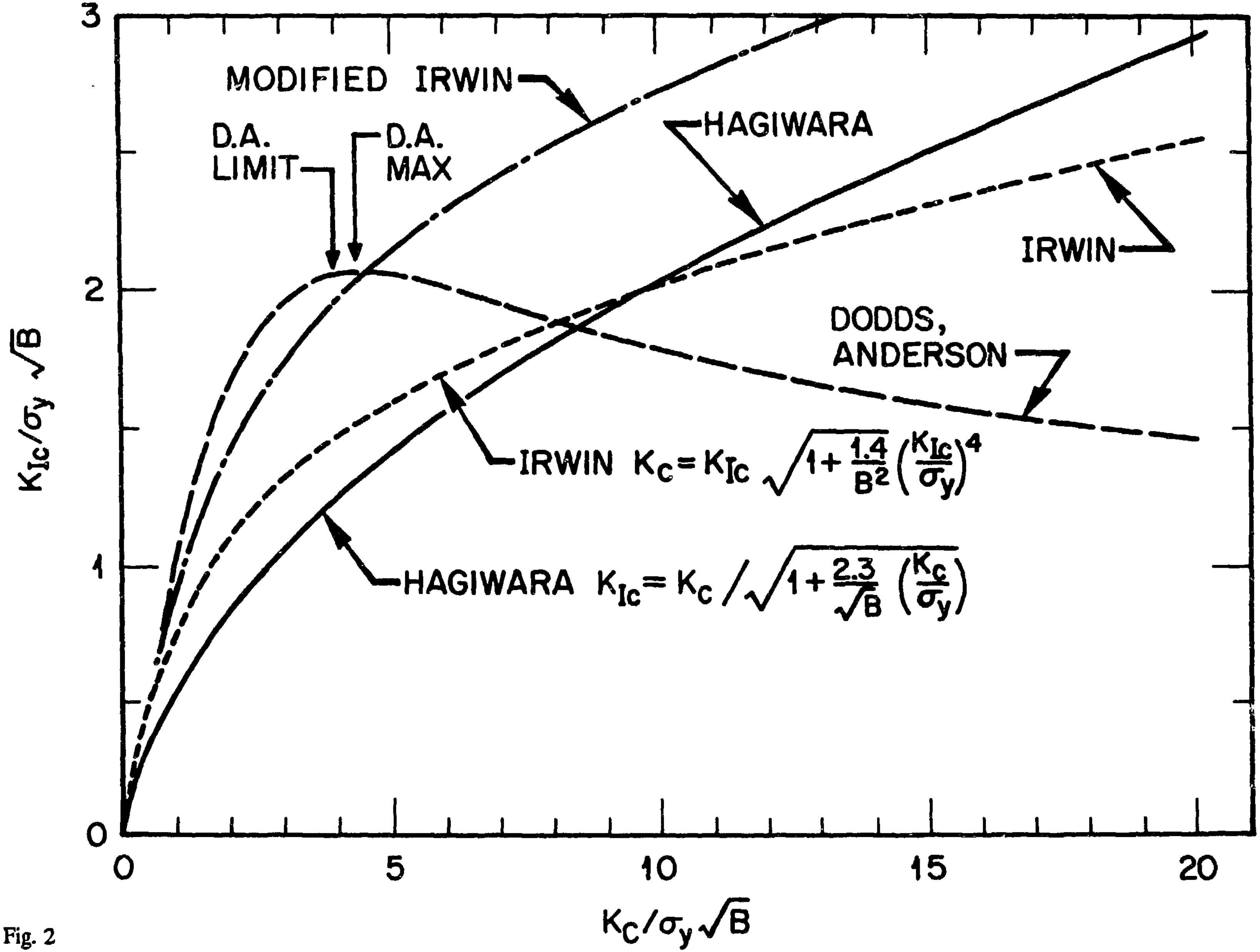

MODIFIED IRWIN
D.A. LIMIT
D.A. MAX
HAGIWARA
IRWIN
DODDS, ANDERSON
IRWIN $K_C = K_{Ic}\sqrt{1+\frac{1.4}{B^2}\left(\frac{K_{Ic}}{\sigma_y}\right)^4}$
HAGIWARA $K_{Ic} = K_C \Big/ \sqrt{1+\frac{2.3}{\sqrt{B}}\left(\frac{K_C}{\sigma_y}\right)}$
$K_{Ic}/\sigma_y\sqrt{B}$
$K_C/\sigma_y\sqrt{B}$
0
1
2
3
5
10
15
20

Fig. 2

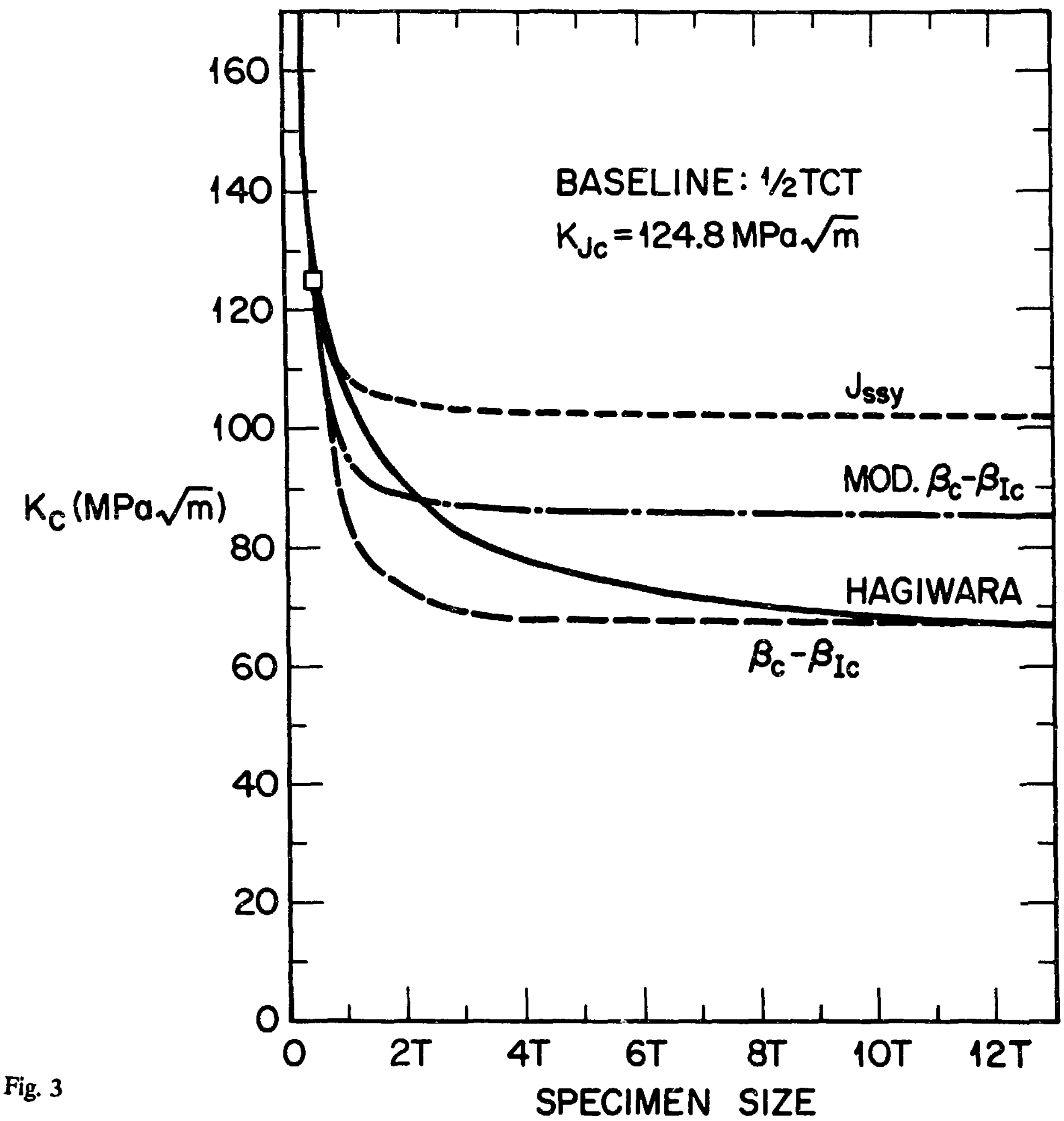
BASELINE: ½TCT
K_{Jc}=124.8 MPa$\sqrt{m}$
J_{ssy}
MOD. β_c-β_{Ic}
HAGIWARA
β_c-β_{Ic}
K_c (MPa$\sqrt{m}$)
160
140
120
100
80
60
40
20
0
0
2T
4T
6T
8T
10T
12T
SPECIMEN SIZE

Fig. 3

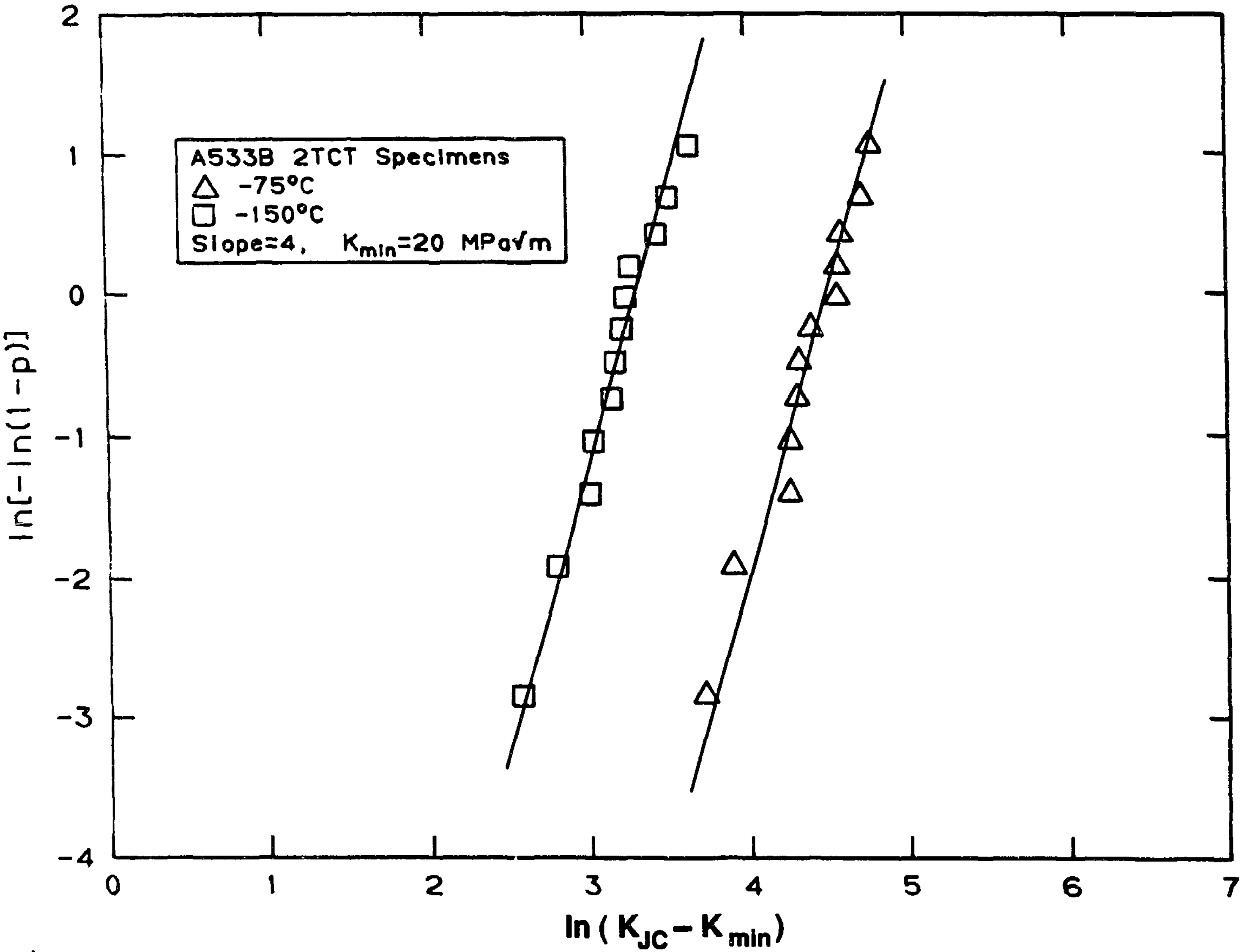

A533B 2TCT Specimens
△ -75°C
□ -150°C
Slope=4, Kmin=20 MPa√m
ln[-ln(1-p)]
ln(KJC-Kmin)
2
1
0
-1
-2
-3
-4
0
1
2
3
4
5
6
7

Fig. 4

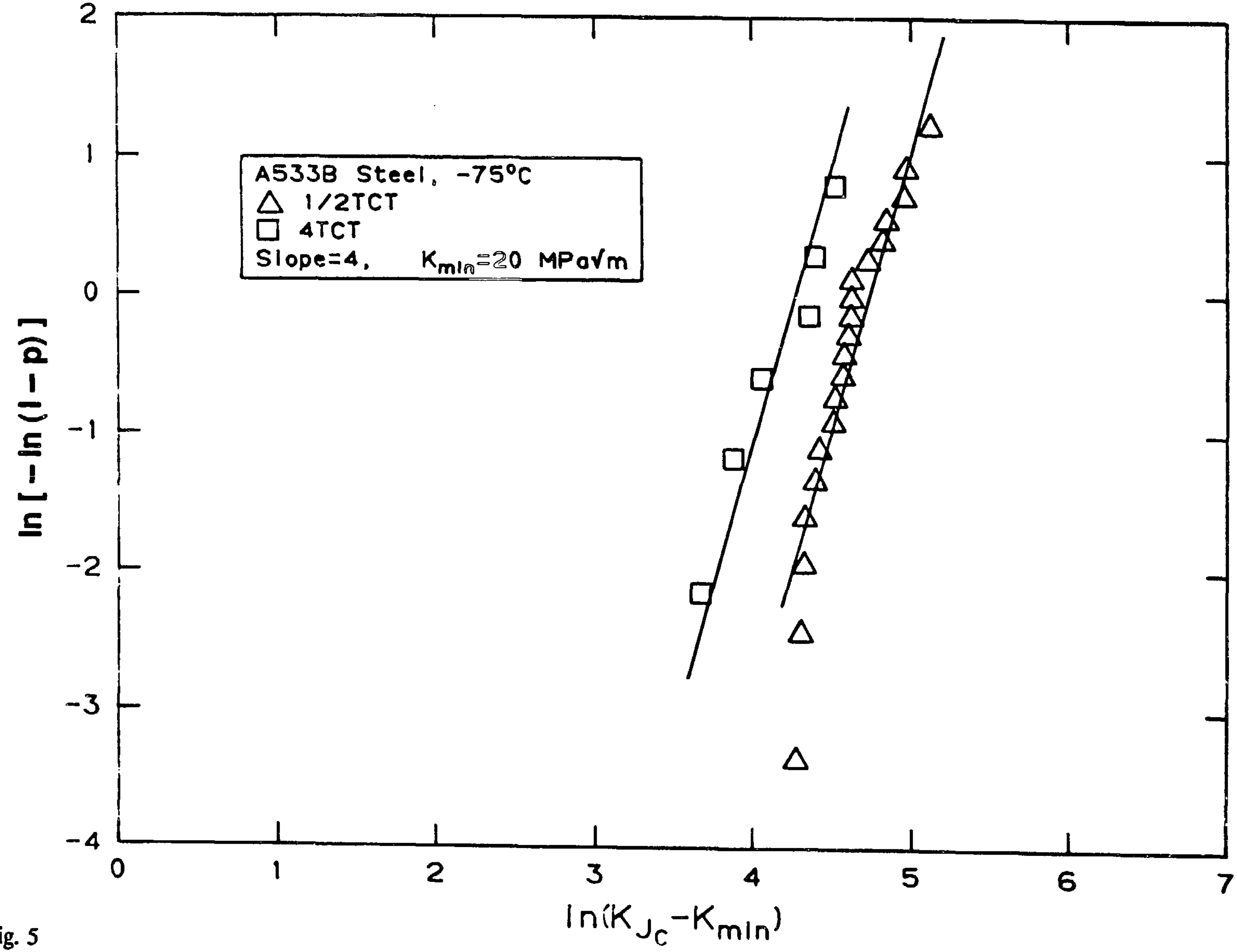
A533B Steel, -75°C
1/2TCT
4TCT
Slope=4, Kmin=20 MPa√m
ln [− ln (1 − p)]
ln(KJc−Kmin)
2
1
0
-1
-2
-3
-4
0
1
2
3
4
5
6
7

Fig. 5

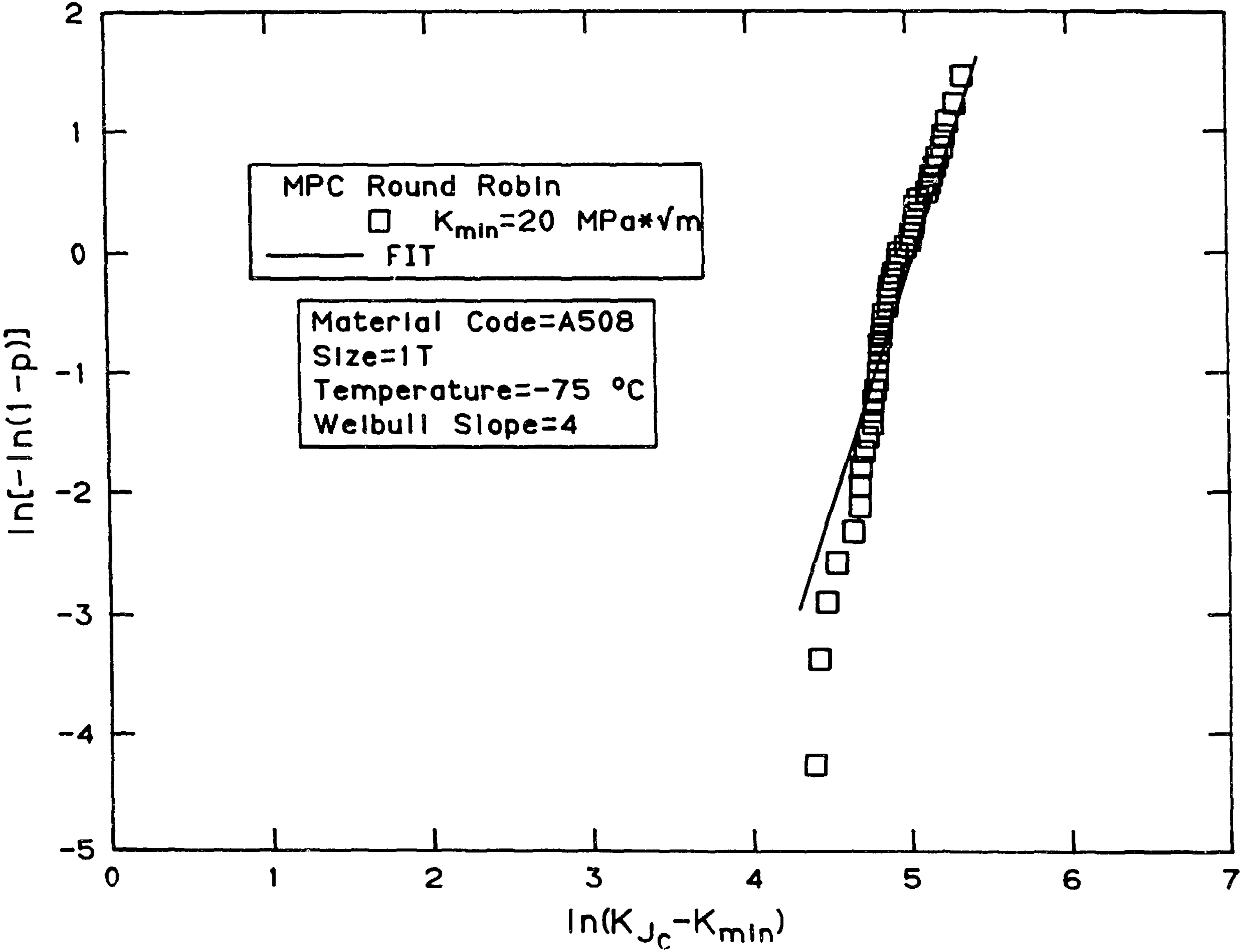

MPC Round Robin
□ Kmin=20 MPa*√m
FIT
Material Code=A508
Size=1T
Temperature=-75 °C
Weibull Slope=4
ln[-ln(1-p)]
ln(KJc-Kmin)
2
1
0
-1
-2
-3
-4
-5
0
1
2
3
4
5
6
7

Fig. 6

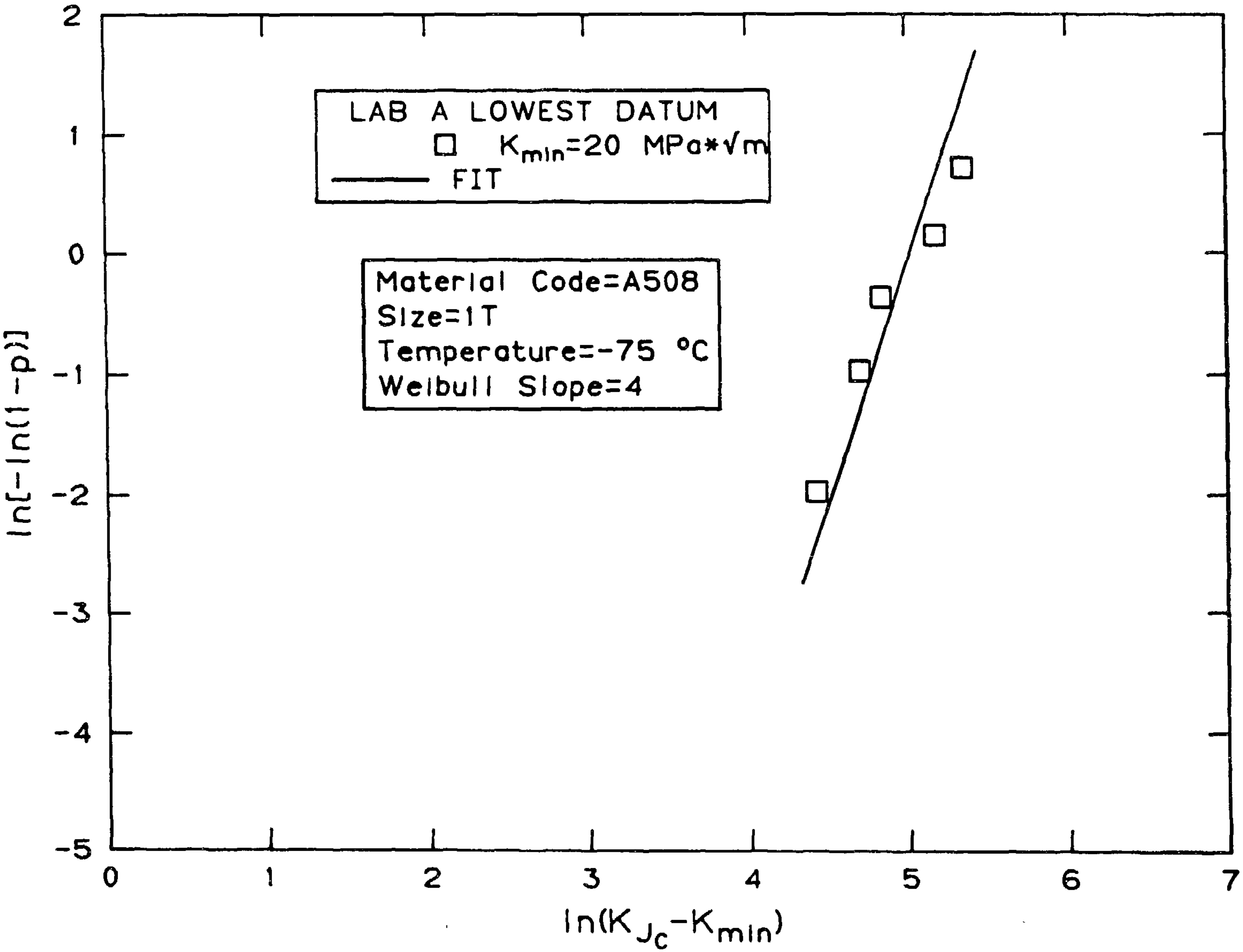

LAB A LOWEST DATUM
K min=20 MPa*√m
FIT
Material Code=A508
Size=1T
Temperature=-75 °C
Weibull Slope=4
ln[-ln(1-p)]
ln(K Jc-K min)
2
1
0
-1
-2
-3
-4
-5
0
1
2
3
4
5
6
7

Fig. 7

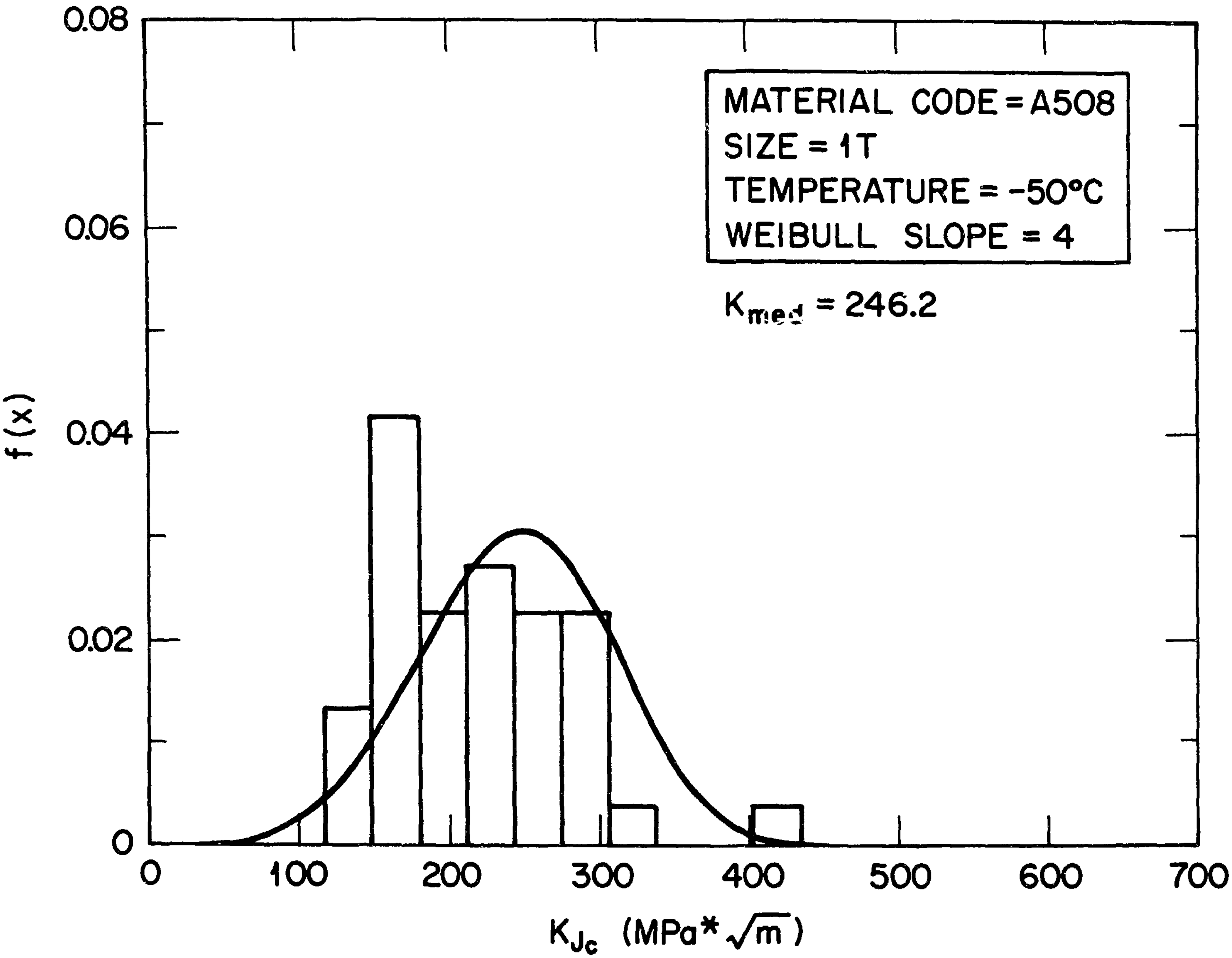

MATERIAL CODE = A508
SIZE = 1T
TEMPERATURE = -50°C
WEIBULL SLOPE = 4
K med = 246.2
f (x)
0.08
0.06
0.04
0.02
0
0
100
200
300
400
500
600
700
K Jc (MPa* √m)

Fig. 8

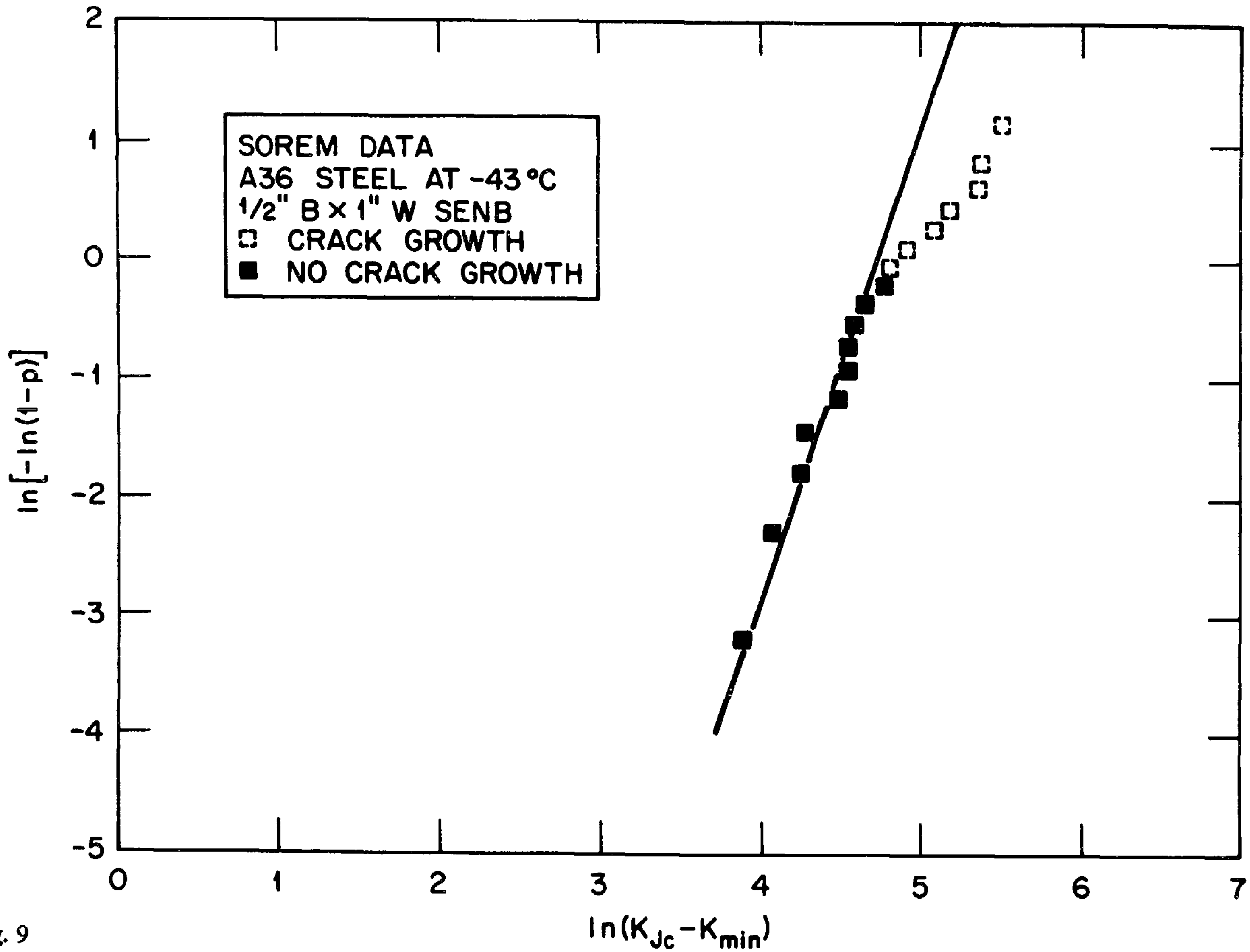
SOREM DATA
A36 STEEL AT -43°C
1/2" B × 1" W SENB
CRACK GROWTH
NO CRACK GROWTH
ln[-ln(1-p)]
ln(K_Jc - K_min)
2
1
0
-1
-2
-3
-4
-5
0
1
2
3
4
5
6
7

Fig. 9

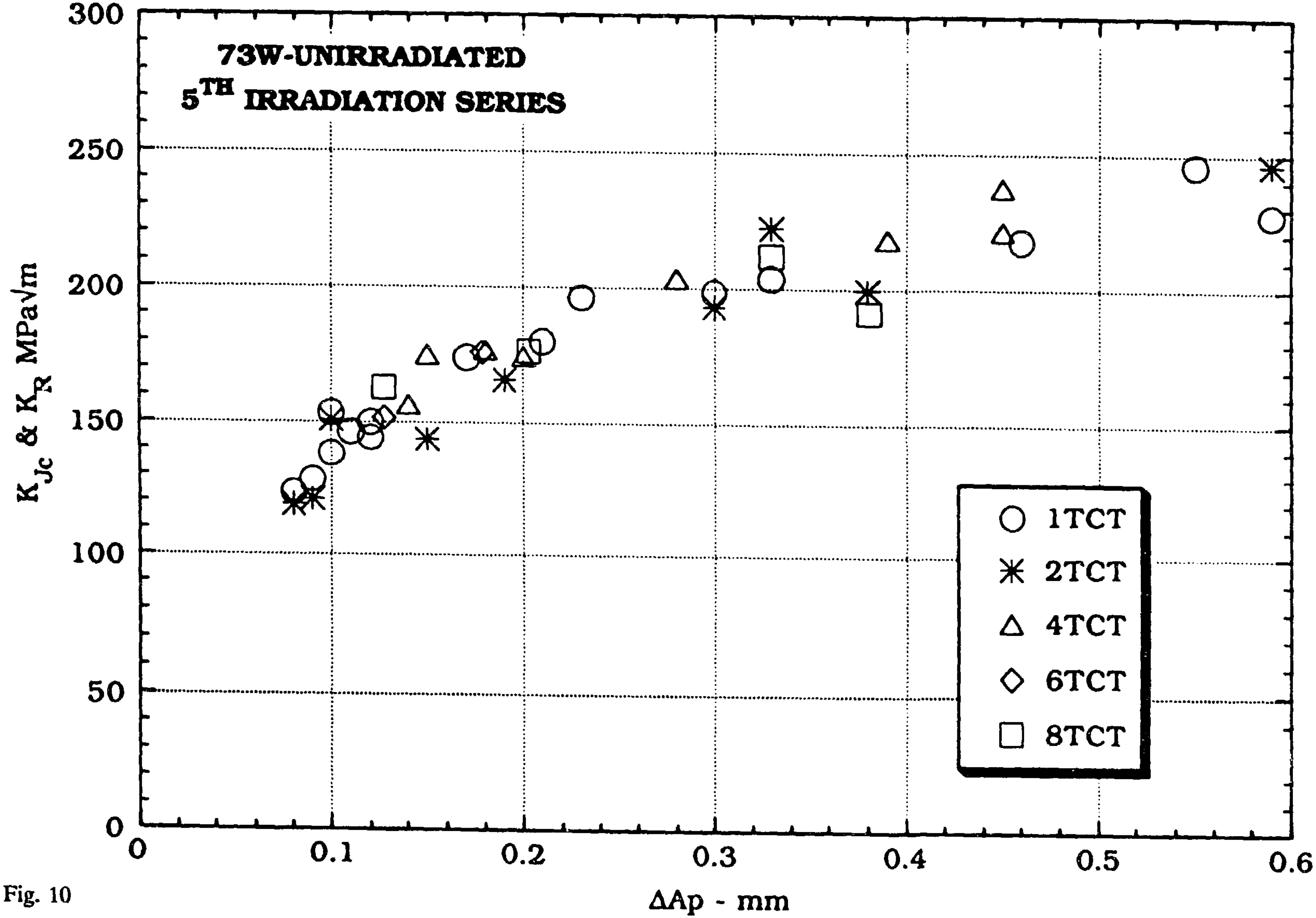

73W-UNIRRADIATED
5TH IRRADIATION SERIES
300
250
200
150
100
50
0
0
0.1
0.2
0.3
0.4
0.5
0.6
K Jc & K R MPa√m
ΔAp - mm
1TCT
2TCT
4TCT
6TCT
8TCT

Fig. 10

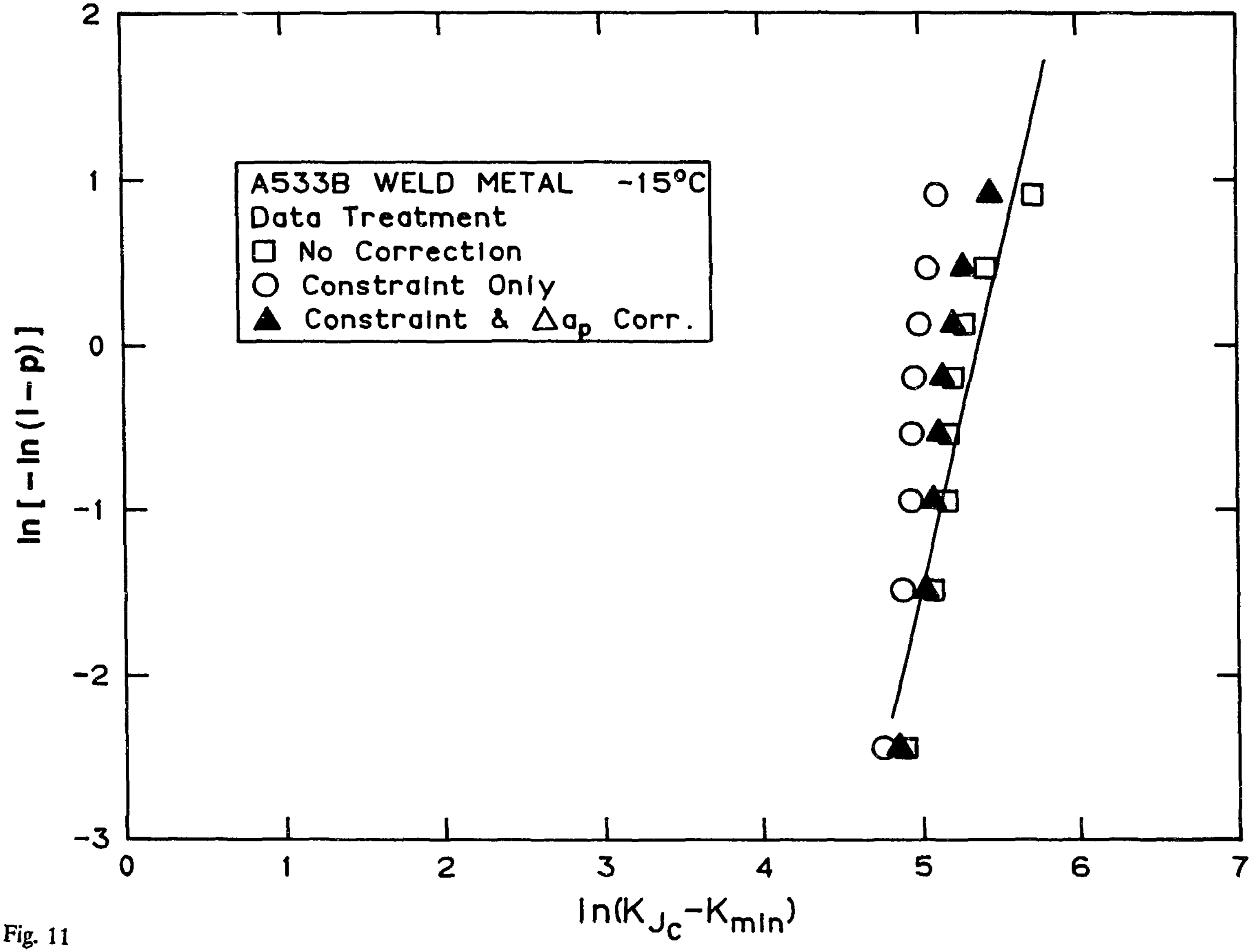
A533B WELD METAL -15°C
Data Treatment
No Correction
Constraint Only
Constraint & Δa_p Corr.
ln[-ln(1-p)]
ln(K_Jc-K_min)
2
1
0
-1
-2
-3
0
1
2
3
4
5
6
7

Fig. 11

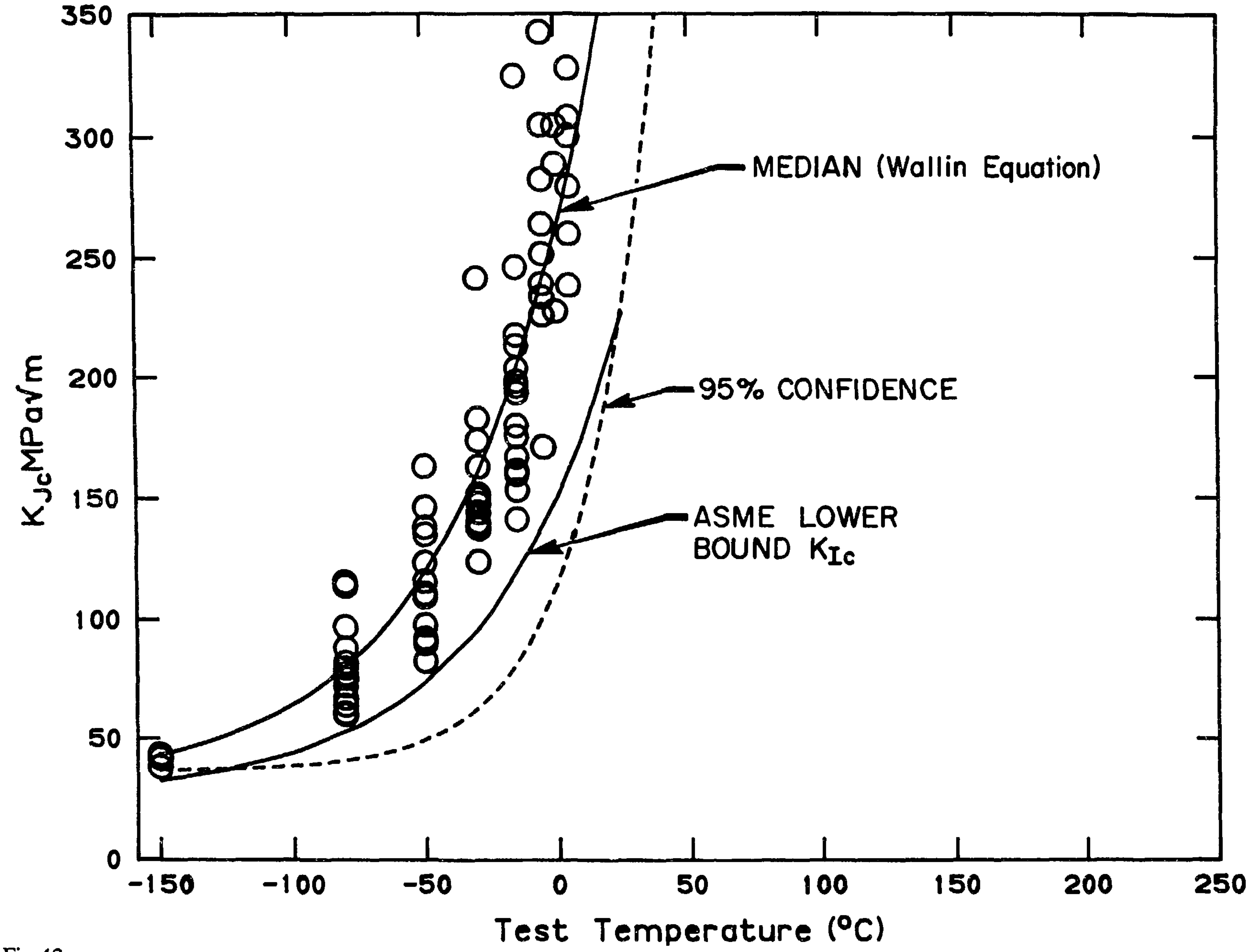

350
300
250
200
150
100
50
0
-150
-100
-50
0
50
100
150
200
250
K Jc MPa√m
Test Temperature (°C)
MEDIAN (Wallin Equation)
95% CONFIDENCE
ASME LOWER
BOUND KIc

Fig. 12